Acta Cryst. (1991). B47, 987–997

Structure of Oligomeric $\beta B2$-Crystallin: an Application of the T_2 Translation Function to an Asymmetric Unit Containing Two Dimers

BY H. P. C. DRIESSEN, B. BAX, C. SLINGSBY, P. F. LINDLEY, D. MAHADEVAN, D. S. MOSS AND I. J. TICKLE

Laboratory of Molecular Biology and Imperial Cancer Research Fund Unit, Department of Crystallography, Birkbeck College, University of London, Malet Street, London WC1E 7HX, England

(*Received* 3 *June* 1991; *accepted* 25 *July* 1991)

Abstract

The molecular structure of the main subunit of the β-crystallins, components of the vertebrate eye lens, has recently been solved by molecular replacement at 2·1 Å resolution [Bax, Lapatto, Nalini, Driessen, Lindley, Mahadevan, Blundell & Slingsby (1990). *Nature* (*London*), **347**, 776–780]. The protein, $\beta B2$, is a dimer in solution, but a tetramer in the crystal with one subunit in the asymmetric unit of space group *I*222. Using the crystallographic dimer from this *I*-centred form the structure of a *C*222 crystal form of the $\beta B2$ protein with four subunits in the asymmetric unit has now been solved by molecular replacement at 3·3 Å. The solution involved the use of a new translation function for non-crystallographic symmetry, based on the T_2 function of Crowther & Blow [*Acta Cryst.* (1967), **23**, 544–548].

Introduction

The β,γ-crystallins form a superfamily of structural proteins in the eye lens. While γ-crystallins are monomeric, β-crystallin subunits associate to form a wide range of oligomers, from dimers upwards. The γ-crystallins comprise four topologically equivalent Greek key motifs, with pairs of motifs organized around a local dyad to give domains (Blundell *et al.*, 1981; Wistow *et al.*, 1983; Chirgadze *et al.*, 1986; White, Driessen, Slingsby, Moss & Lindley, 1989). Two similar domains are in turn related by a further dyad, and are linked by a short connecting peptide (Fig. 1*a*). Based on the sequence homology the structure of β-crystallin subunits was predicted to be similar, but with N- and C-terminal extensions or arms (Wistow, Slingsby, Blundell, Driessen, de Jong & Bloemendal, 1981; Slingsby, Driessen, Mahadevan, Bax & Blundell, 1988). β-Crystallins comprise a multigene family of basic ($\beta B1$, $\beta B2$, $\beta B3$) and acidic ($\beta A1$, $\beta A2$, $\beta A3$, $\beta A4$) polypeptides (Berbers, Hoekman, Bloemendal, de Jong, Kleinschmidt & Braunitzer, 1984). The individual chains have between 45 and 60% identity with each other for the regions corresponding to the two globular domains, but only some 30% sequence homology with the γ-crystallins.

The simplest β-crystallin aggregate is a homodimer of two $\beta B2$ subunits. The structure of an *I*222 crystal form of the $\beta B2$ homodimer, which contains only one subunit (*i.e.* half a dimer) in the asymmetric unit, has recently been solved at 2·1 Å by molecular replacement (Bax *et al.*, 1990). The structure confirms the predictions about the globular domains,

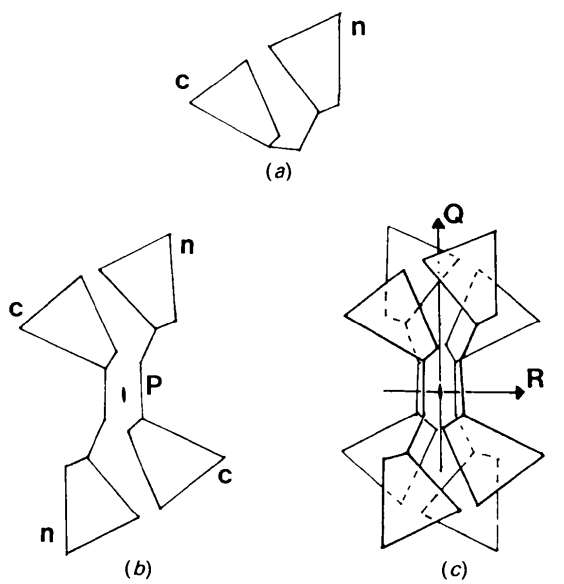

Fig. 1. Schematic diagrams showing the structure of proteins with definition of axes and interfaces. Domains are shown as wedges, and labeled as N- or C-terminal. (*a*) Monomeric γ-crystallin. γ-Crystallins consist of two homologous domains, closely interacting around a pseudo twofold axis and linked by a short connecting peptide. (*b*) $\beta B2$ dimer. In the $\beta B2$ dimer the domain–domain interactions are similar to those found in monomeric γ-crystallins. However, these interactions are intersubunit rather than intra-subunit. In the *I*222 form the two subunits are related by a crystallographic twofold axis *P* perpendicular to the page. (*c*) $\beta B2$ tetramer. In the *I*222 form there are extensive interactions between two dimers around the vertical crystallographic twofold axis *Q* which together with the horizontal twofold *R* gives a tetramer with 222 symmetry. The search molecule used to solve the *C*222 form consisted of the four non-covalently linked domains above the *PR* plane, which can be viewed as a 'dimer' of γ-like subunits.

0108-7681/91/060987-11$03.00

but shows that the connecting peptide is extended and the two domains separated in a way quite unlike γ-crystallins. Domain interactions analogous to those within monomeric γ-crystallins are intermolecular and related by a crystallographic dyad *P* in the βB2 dimer (Fig. 1*b*). In the crystal lattice two dimers aggregate around further dyads *Q* and *R* to give a tetramer with 222 symmetry (Fig. 1*c*).

βB2 was originally crystallized in the early 1980's (Slingsby, Miller & Berbers, 1982) in a relatively large unit cell [$a = 154{\cdot}7\,(2)$, $b = 165{\cdot}9\,(3)$, $c = 78{\cdot}48\,(8)$ Å], with four subunits in the asymmetric unit of space group *C*222. Attempts to solve this structure using conventional molecular replacement methods were unsuccessful. The solution of the structure of these *C*-form crystals using the dimer of the *I* form as a search model is described herein. It confirms the unexpected connectivity seen in the *I*-form dimer, and in addition demonstrates that βB2 dimers (and tetramers) have a limited degree of flexibility.

Derivation of the non-crystallographic translation function

The translation function used in this work is essentially the T_2 function of Crowther & Blow (1967) which is based on the work of Tollin (1966); see also Tollin (1969). This dealt with the case of only one molecule with an unknown translation vector in the crystallographic asymmetric unit. Here an extension of this concept to the case of non-crystallographic symmetry, where there are several protein subunits each with an unknown translation vector in the crystallographic asymmetric unit, is described.

The translation function *T* was defined by Crowther & Blow (1967) as the product function:

$$T(\mathbf{t}) = \int_V P_o(\mathbf{u})\,P_{kl}(\mathbf{u},\mathbf{t})\,\mathrm{d}\mathbf{u}.$$

Here P_o is the observed Patterson function (of the vector **u**) for the structure to be solved. P_{kl} is the calculated cross-Patterson function between the molecules being used as a search model in general equivalent positions *k* and *l*, whose atomic coordinates are initially specified relative to some arbitrary local origin (typically the molecular centroid); **t** is the unknown intermolecular vector between the local origins of molecules *k* and *l*. The integration is over the unit-cell volume *V*. The correct intermolecular vector should correspond to a maximum in the correlation between the observed and calculated Pattersons and hence a maximum in the *T* function.

Crowther & Blow's *T* function is applied to only one pair of molecules at a time, and therefore produces a two-dimensional translation function, since for chiral space groups only rotation and screw-axis symmetry elements need be considered. The T_2 function is, in general, a three-dimensional sum function of the individual two-dimensional *T* functions. In low-symmetry space groups the task of correlating a small number of such sections is straightforward, but in high-symmetry space groups it becomes more complicated. Moreover, the solution peak may well not be the highest in each section and may only become apparent when the sum function is performed. This is particularly true when there is a considerable lack of homology between the model and unknown structures, as is often the case. Wilson & Tollin (1988) introduced a correlation procedure as an improvement over this straight sum function, but we have found that in practice the latter always gives the correct result and for high-symmetry space groups has considerable computational advantages.

In this work Crowther & Blow's T_2 function with subtraction of all known vectors is used:

$$T_2(\mathbf{t}_1,\mathbf{t}_2,\ldots) = \int_V [P_o(\mathbf{u}) - P_m(\mathbf{u})] \times [P_c(\mathbf{u},\mathbf{t}_1,\mathbf{t}_2,\ldots) - P_m(\mathbf{u})]\,\mathrm{d}\mathbf{u}.$$

Here $\mathbf{t}_1,\mathbf{t}_2,\ldots$ are the translation vectors (not the vector between the molecular origins defined by Crowther & Blow) for the subunits in the asymmetric unit generated by the crystallographic space-group identity operator. P_c is the total calculated Patterson function, and P_m is the calculated Patterson function for all known vectors; that is, not only intra-subunit vectors as in the original T_2 function but also vectors between subunits whose positions are already known. Hence $[P_c - P_m]$ represents all the unknown vectors.

By subtracting intra-subunit and known inter-subunit vectors from the observed Patterson synthesis, we take account of overlap between the atoms in different subunits of the model and reduce the 'noise' in the translation function. It is a common belief that the T_2 function does not take account of such overlap, and therefore that the function needs to be modified by further 'packing' terms (Harada, Lifchitz, Berthou & Jolles, 1981). However, consider the following argument: the $[P_o - P_m]$ Patterson has very little density close to, and at, the origin because all the short intra-subunit vectors have been removed; the $[P_c - P_m]$ Patterson consists of sets of peaks which move relative to each other as the translation vectors are varied, but do not change height unless different sets happen to overlap. We seek to maximize the sum of products of the two Patterson syntheses. If the atoms of the model overlap, then the $[P_c - P_m]$ density will accumulate in the neighbourhood of the origin, and will be correspondingly reduced elsewhere; hence the sum of products will be small and no peak in the translation function will be observed. Only when there are no

short inter-subunit vectors can the Patterson syntheses correlate well and the T_2 function be maximal.

Except in space group $P1$, where the position of the first subunit in the asymmetric unit can be chosen arbitrarily, and in polar space groups where the axial coordinate of the first subunit is arbitrary, nothing will be known initially about the positions. The strategy is to proceed in a stepwise fashion, determining the positions of the subunits one at a time and then using the information gained to determine the positions of the other subunits. Ideally one would like to set up a function of all the unknown translation vectors simultaneously, as suggested by Vagin (1989), but for four subunits, for example, this would require the use of a 12-dimensional Fourier transform, and this is not a practical proposition.

The T_2 function is transformed into reciprocal space by application of Parseval's theorem (Whittaker & Watson, 1927):

$$T_2(\mathbf{t}_1,\mathbf{t}_2,\ldots) = \sum_{\mathbf{h}} [\,|E_o(\mathbf{h})|^2 - |E_m(\mathbf{h})|^2] \times [\,|E_c(\mathbf{h},\mathbf{t}_1,\mathbf{t}_2,\ldots)|^2 - |E_m(\mathbf{h})|^2].$$

Here E_o, E_m and E_c are the normalized structure amplitudes corresponding to the observed, known and total calculated Patterson functions. E's are used here rather than F's, because otherwise the scattering and thermal factor fall-offs inherent in the F's are raised to the fourth power in the T_2 function and obliterate the high-resolution data needed for sensitivity of the function to small changes in the translation vectors. This idea was originally suggested by Tollin (1966), and implemented for macromolecules by Harada, Lifchitz, Berthou & Jolles (1981); see also Tickle (1985). In practice the E's for the model structure are not calculated directly, but by normalizing the $F_{\rm calc}$'s, since then allowance can be made for differing scattering and, in particular, thermal factors. This also solves the problem of scaling the $F_{\rm obs}$ and $F_{\rm calc}$ together, since the use of E's automatically places them on a common scale.

In order to determine the known part F_m, the total calculated structure factor F_c needs to be obtained first. This can be written as the sum of the structure factor F_P for the set of subunits whose positions (if any) have been previously determined, the structure factor F_x for the subunit whose position is to be determined in the current pass together with its crystallographic equivalents, and the structure factor F_U for the remaining set of subunits whose positions are as yet unknown:

$$F_c(\mathbf{h},\mathbf{t}_1,\mathbf{t}_2,\ldots) = F_P(\mathbf{h},\mathbf{P}) + F_x(\mathbf{h},\mathbf{t}_x) + F_U(\mathbf{h},\mathbf{U}).$$

Here $\mathbf{P}$ is the set of previously determined translation vectors, $\mathbf{t}_x$ is the unknown translation vector to be determined, and $\mathbf{U}$ is the set of remaining unknown translation vectors, so that

$$\{\mathbf{t}_1,\mathbf{t}_2,\ldots\} = \mathbf{P} + \{\mathbf{t}_x\} + \mathbf{U}.$$

$\mathbf{P}$ and/or $\mathbf{U}$ may be empty sets. Then:

$$\begin{aligned}|F_c(\mathbf{h},\mathbf{t}_1,\mathbf{t}_2,\ldots)|^2 &= F_c(\mathbf{h},\mathbf{t}_1,\mathbf{t}_2,\ldots)F_c(\mathbf{h},\mathbf{t}_1,\mathbf{t}_2,\ldots)^* \\ &= |F_P(\mathbf{h},\mathbf{P})|^2 + |F_x(\mathbf{h},\mathbf{t}_x)|^2 + |F_U(\mathbf{h},\mathbf{U})|^2 \\ &\quad + \mathrm{Re}[2F_P(\mathbf{h},\mathbf{P})F_x(\mathbf{h},\mathbf{t}_x)^*] \\ &\quad + \mathrm{Re}[2F_P(\mathbf{h},\mathbf{P})F_U(\mathbf{h},\mathbf{U})^*] \\ &\quad + \mathrm{Re}[2F_x(\mathbf{h},\mathbf{t}_x)F_U(\mathbf{h},\mathbf{U})^*].\end{aligned}$$

The first term in this expansion represents the vector set (intra- and inter-subunit) between the known subunits and can be calculated directly; the second and fourth terms have to be expanded further in terms of $\mathbf{t}_x$. The other terms depend on the other unknown translation vectors, and the best that can be done is to replace them by their expectation values; for the last two terms this is zero.

The unknown F_x is the sum of the structure factors for the crystallographically equivalent subunits with translation vectors $\mathbf{t}_{xk}$:

$$F_x(\mathbf{h},\mathbf{t}_x) = \sum_k F_{xk}(\mathbf{h})\exp(2\pi i\,\mathbf{h}.\mathbf{t}_{xk}).$$

This shows that the partial structure factors need only be calculated once, independently of the translations (Nixon & North, 1976). Hence:

$$\begin{aligned}|F_x(\mathbf{h},\mathbf{t}_x)|^2 &= \sum_k\sum_l F_{xk}(\mathbf{h})F_{xl}(\mathbf{h})^*\exp[2\pi i\mathbf{h}.(\mathbf{t}_{xk}-\mathbf{t}_{xl})] \\ &= \sum_k |F_{xk}(\mathbf{h})|^2 + \mathrm{Re}\{2\sum_k\sum_{l<k} F_{xk}(\mathbf{h})F_{xl}(\mathbf{h})^* \\ &\quad \times \exp[2\pi i\mathbf{h}.(\mathbf{t}_{xk}-\mathbf{t}_{xl})]\}.\end{aligned}$$

The first term here represents the intra-subunit vectors for subunit x and its equivalents and is independent of the translations; the second term represents the crystallographic inter-subunit vectors.

The term $|F_U(\mathbf{h},\mathbf{U})|^2$ can be similarly expanded into intra- and inter-subunit terms, but in this case the translation vectors are unknown, so the inter-subunit term is replaced by its expectation value, which is zero.

Now expanding the cross-term, which represents inter-subunit vectors between non-crystallographically related subunits:

$$F_P(\mathbf{h},\mathbf{P})F_x(\mathbf{h},\mathbf{t}_x)^* = F_P(\mathbf{h},\mathbf{P})\sum_k F_{xk}(\mathbf{h})^*\exp(-2\pi i\mathbf{h}.\mathbf{t}_{xk}).$$

In these expressions, the translation vector $\mathbf{t}_{xk}$ for the kth asymmetric unit has to be expressed in terms of $\mathbf{t}_x$, the translation vector for the asymmetric unit generated by the identity operation:

$$\mathbf{t}_{xk} = A_k.\mathbf{t}_x + \mathbf{d}_k,$$

where A_k and $\mathbf{d}_k$ are the rotational and translational components of the kth space-group operator.

Thus the total contribution to the vector set involving the subunit whose position is to be

determined, together with its crystallographic equivalents, is:

$$\mathrm{Re}(2\sum_k\sum_{l<k}F_{vk}(\mathbf{h})F_{vl}(\mathbf{h})^* \times \exp\{2\pi i\mathbf{h}.[(A_k - A_l).\mathbf{t}_v + \mathbf{d}_k - \mathbf{d}_l]\}) + \mathrm{Re}\{2F_P(\mathbf{h},\mathbf{P})\sum_k F_{vk}(\mathbf{h})^*\exp[-2\pi i\mathbf{h}.(A_k.\mathbf{t}_v + \mathbf{d}_k)]\}.$$

Here the first term represents the crystallographic inter-subunit vector contribution. Although Crowther & Blow (1967) stated that this could not be computed as a Fourier series using **h** as the index vector, Harada, Lifchitz, Berthou & Jolles (1981) pointed out that this is in the form required of a Fourier coefficient if $-\mathbf{h}.(A_k - A_l)$ is taken as the index vector. The second term represents the non-crystallographic inter-subunit vector contribution and when multiplied by the $|F_o|^2$ term in the T_2 function expression is essentially the 'phased translation function' of Read & Schierbeek (1988), except that there the partial structure factor was derived from an uninterpretable MIR map, rather than from part of the same structure already determined using the translation function. In this case computation by Fourier transform can be performed using $\mathbf{h}.A_k$ as the index vector.

The contribution for the complete set of known, including intra-subunit, vectors is:

$$|F_m(\mathbf{h})|^2 = |F_P(\mathbf{h},\mathbf{P})|^2 + \sum_k|F_{vk}(\mathbf{h})|^2 + \sum_l\sum_k|F_{lk}(\mathbf{h})|^2.$$

This is normalized and subtracted from the normalized squared observed amplitude to form the $[|E_o|^2 - |E_m|^2]$ term in the T_2 function expression. The normalized squared amplitude is just the ratio of the squared amplitude to the average taken in equi-volume shells in reciprocal space. The terms representing all the inter-subunit vectors to be determined are added and normalized to form the $[|E_c|^2 - |E_m|^2]$ term. This second normalization is simplified because the expectation value of $|F_c|^2$ is just $|F_m|^2$.

It can be seen that the index vector for the Fourier series in the crystallographic contribution, $-\mathbf{h}.(A_k - A_l)$, is a projection in reciprocal space, and therefore does not bear a unique relationship to the original index vector **h**. However, for the non-crystallographic component the index vector, $\mathbf{h}.A_k$, is just the symmetry-expanded index. Because the sets of indices are different for the two components, it is convenient to compute the Fourier coefficients of the crystallographic and non-crystallographic contributions to the translation function with separate programs, perform the Fourier transforms using the *FFT* algorithm (Ten Eyck, 1973) and finally add the contributions together in real space.

The crystallographic translation function has non-primitive lattice translations due to the alternative origin positions of the actual space group. For example, in orthorhombic space groups these origin positions are at 0 and $\frac{1}{2}$ in x, y and z, which reduces the asymmetric unit to 0 to $\frac{1}{2}$ along each axis. In chiral space groups these alternative origins arise either from rotational or non-primitive lattice symmetry elements. The non-crystallographic translation function only has translational symmetry arising from the lattice-centring symmetry elements, so that the whole primitive cell must be computed. For $P2_1$ the crystallographic and non-crystallographic asymmetric units are ($x = 0$–$\frac{1}{2}$, $y = 0$, $z = 0$–$\frac{1}{2}$) and the whole cell respectively.

Programs to compute the Fourier coefficients of the crystallographic and non-crystallographic translation functions, *TFSGEN* and *TFPART* respectively, have been written by one of us (IJT). The program to perform the addition of the translation function maps and search for significant peaks is *MAPSIG*. These are publicly available in the *CCP*4 suite (*CCP*4, 1979). *MAPSIG* automatically expands the crystallographic asymmetric unit to the size of the non-crystallographic asymmetric unit.

Experimental

Native data collection and processing

The original *C*222 (*C*-form) crystals were grown at 277 K and were unstable to X-rays at room temperature. The crystals were therefore cooled to 268 K during data collection. A native data set was collected on film using an Arndt–Wonacott oscillation camera. The crystals were mounted so that c axis was parallel to the rotation axis. A total of four symmetry equivalents were measured excluding the cusp region. Data were collected from six crystals on a rotating-anode generator operating at 40 kV and 35 mA. Ni-filtered Cu $K\alpha$ radiation (λ = 1·5418 Å) was used with a crystal-to-film distance of 80 mm. In each case 2° oscillation steps were used, and three films (Ceaverken Reflex 25) were included in each filmpack to give a satisfactory dynamic range.

The photographs were digitized on a Joyce–Loebl Scandig 3 microdensitometer under on-line control of a Data General Nova 3/12 computer. All scanning was performed using a 50 μm raster step and an optical density range of 0·0–2·0 units. The digitized data were processed with the *MOSFILM* suite (Leslie, Brick & Wonacott, 1986). The inter-filmpack scaling was performed using the scaling algorithm of Fox & Holmes (1966) where a refinable scale and temperature factor are assigned to each film using the *CCP*4 programs *ROTAVATA* and *AGROVATA* (*CCP*4, 1979). Parameters were further refined using *POSTREF* (Winkler, Schutt & Harrison, 1979; *CCP*4, 1979). Amplitudes were produced with *TRUNCATE* (French & Wilson, 1978; *CCP*4, 1979).

Scaling and merging of 57 643 observations including 13 188 partially recorded reflections gave a residual of 10·6% for 14 922 unique reflections to 3·3 Å. The data are 95·6% complete to this resolution, and are still 89·7% complete between 3·53 and 3·30 Å. The number of measurements $>3\sigma$ was 80%. No absorption corrections were applied.

Rotation function

For the cross-rotation the search molecule was generated from the 2·65 Å coordinates of the bovine $\beta B2$-crystallin *I* form (Bax *et al.*, 1990). A dimer of γ-type monomers was generated from a single γ-like subunit using the symmetry of the *I*-centred cell (Fig. 1*c*). The internal twofold of the dimer was parallel to the *z* axis and positioned at the origin ($x = y = 0{\cdot}0$) of an orthogonal cell of *P*1 symmetry with dimensions $a = b = 80$, $c = 60$ Å. Structure factors were calculated to 3·3 Å using the atomic temperature factors of *I*-form $\beta B2$ with *GENSFC* (*CCP*4, 1979), incorporating the *FFT* program (Ten Eyck, 1973).

Cross-rotation searches were performed with *ALMN* (*CCP*4, 1979), based on Crowther's (1972) fast-rotation function. Normalized structure-factor amplitudes were used for search molecule and measured native data. An initial map was calculated using 5° steps in each of the Eulerian angles α, β and γ (30 Bessel functions). In the region of relevant peaks the resolving power was extended to a step size of 2·5° in all angles (60 Bessel functions). The maps were investigated with 9000 reflections in the resolution range 3·3–20·0 Å, a Patterson radius of 18·0 Å and origin cut-off of 6·0 Å. Self-rotation searches were performed with *POLARRFN* (*CCP*4, 1979), a modification of Crowther's fast-rotation function by Kabsch. Normalized structure-factor amplitudes were used. Maps were calculated using 5° steps (30 Bessel functions) for 6000 reflections in the resolution range 3·3–20·0 Å, and Patterson radii of 15·0, 18·0 and 21·0 Å.

The rotation functions are sampled at equally spaced intervals of the Eulerian angles (α, β, γ) for the cross-rotation and polar angles (θ, φ, χ) for the self-rotation. In neither case do the sample points represent equal volumes of the sample space. Estimates of the standard deviations of the functions, which are used to evaluate the significance of the peaks, are therefore computed as the root weighted mean-square function value, where the weight factor is given by $\sin\beta$ and $\sin\theta(1-\cos\chi)$ for the Eulerian and polar angles respectively. For mirror and glide planes of symmetry in the functions there is also a symmetry factor of 0·5 for each plane, provided only one asymmetric unit is used in the calculation. In the present work, the symmetry planes are at $\beta = 0$ and $\pi/2$ in the cross-rotation function, and at $\theta = 0$, $\pi/2$, $\varphi = 0$, $\pi/2$, $\chi = 0$, π in the self-rotation function. As a check that the weight factors are correct, the weighted mean was also computed and found to be zero ($\pm 0{\cdot}1\%$ of the origin peak height). This is expected because the zero-order Fourier coefficients were omitted in the rotation-function calculations.

Translation function

The two rotation-function solutions found for *C*-$\beta B2$ (peaks *A*1 and *B*1) were applied to the model *I*-$\beta B2$ coordinates. The two search models were then optimized by removing residue −1 and the connecting peptide residues 84–87 [the numbering is based on Bax *et al.* (1990)]. Each dimer was put into an orthogonal cell of *P*1 symmetry with the dimensions of the *C* form, and structure factors were calculated to 3·3 Å, using the atomic temperature factors of the *I* form, with *GENSFC*. Partial structure factors were calculated for each symmetry-related molecule in *C*222 using the *PREPARE-COLLATE-MERGE* steps (*CCP*4, 1979). As no space-group translations were applied the partial structure factors could be used for translation functions in both *C*222 and $C222_1$.

Maps were calculated in space group *C*222 using data between 3·3 and 20·0 Å with a 0·8 Å step size. The translational parameters for each of the two independent dimers in the crystallographic asymmetric unit were determined stepwise. Initially the translation vector for dimer *B*1 inside the crystallographic asymmetric unit of the translation function was determined using *TFSGEN* with intra-dimer vectors for dimers *A*1 and *B*1 subtracted. The position of *B*1 was input to the following calculations, to determine the translation of dimer *A*1 with respect to the same origin. The vector for dimer *A*1 relative to one of the four crystallographic equivalent origins was determined with *TFSGEN*, and relative to the same origin as dimer *B*1 with *TFPART*. The two were summed with *MAPSIG* to give the final translation parameters of dimer *A*1. The same procedure was repeated for space group $C222_1$. Packing was studied graphically using *MOLPACK* (Wang, Driessen & Tickle, 1991).

Results and discussion

Space group

$\beta B2$ was originally crystallized in the early 1980's (Slingsby, Miller & Berbers, 1982) in a relatively large unit cell [$a = 154{\cdot}7$ (2), $b = 165{\cdot}9$ (3), $c = 78{\cdot}48$ (8) Å], with four molecules in the asymmetric unit. The space group was reported as $C222_1$ because of a systematic absence along the *c* axis ($00l$, $l = 2n$), while the presence of a pseudo-tetragonal cell was noted. However, if the space group is *C*222 the

presence of a pseudo 4_2 axis could alternatively explain the absence. In order to test the extent of the pseudo fourfold axis in reciprocal space, an *F*-ratio test was performed testing the hypothesis that $F(hkl)$ and $F(khl)$ are drawn from the same population. The test showed that the fourfold axis is indeed present to the highest-resolution data available, although stronger at low resolution. A systematic absence along the $hh0$ axis ($h = 2n$ at low resolution) suggested that the pseudo space group is $P4_22_12$ rather than $P4_222$.

Therefore the space group was more likely $C222$ with the systematic absence along the c axis caused by a pseudo 4_2 axis in a primitive pseudo $P4_22_12$ cell ($a = b = 113$, $c = 78{\cdot}48$ Å, $\alpha = \beta = 90$, $\gamma = 93$).

Determination of the rotational parameters

Self rotation. The self-rotation for the *C* form is very complicated because of the presence of four molecules in the asymmetric unit. There may be three levels of fit, as the asymmetric unit contains two dimers which can be viewed as four monomers or eight domains. The height of the respective peaks will decrease in that order. Suppose only dimers give peaks, then for $C222$ for dimers *A* and *B* there will be expected $2 \times 4 = 8$ orientations giving rise to 64 peaks. Of these rotations 32 are crystallographic twofolds or identity operators. The self-rotation function has *mmm* symmetry and only four of the remaining 32 peaks will occur in the asymmetric unit of the self-rotation function. However, because both dimers possess internal twofolds, there will be four such sets of dimer onto dimer peaks: *A* onto *B*, *A* onto *B'*, *A* onto *A'* and *B* onto *B'* (where *A'* is dimer *A* with the monomers rotated around the internal twofold of the dimer). In the asymmetric unit of the self-rotation function there will be $4 \times 4 = 16$ peaks representing dimer onto dimer rotations. The result of the presence of so many peaks in the rotation functions will be a complicated map, where peaks may overlap and coalesce. The presence of cross-vectors is also likely to reduce the resolving power further.

The self-rotation is dominated by dimer onto dimer rotations, which represent the pseudo space group. Using *E*'s in a resolution shell of 3·3–20·0 Å, there are two equally high peaks (Fig. 2, Table 1). The first peak, with $\chi = 90{\cdot}0$, which reflects the pseudo fourfold, is found on a special position parallel to the z axis. It represents several rotations, which are not resolved. The second equally high peak is also on a special position, at $\chi = 180{\cdot}0$, parallel to the diagonal of the *C* cell. It corresponds to the rotation component of the 2_1 axis in the pseudo-cell. This peak also consists of several rotations, which are not resolved.

Cross-rotation with the βB2 dimer. The first attempt to solve the structure used one *γB* monomer as the search molecule in a similar manner to that reported for γIVa crystallin (White, Driessen, Slingsby, Moss, Turnell & Lindley, 1988). However, it was not successful, as peak positions in the cross-rotation were not accurate enough. The *γB* model, 30% homologous with *βB2*, and incomplete because of the absence of the N- and C-terminal extensions, represented less than $\frac{1}{4}$ of the target. The solution of the *I*-form structure of the *βB2*-dimer model gave a much better chance of solving the *C* structure. The three-dimensional structure is much closer, the presence of half the structure in the asymmetric unit gives a better signal-to-noise ratio, and the cross-rotation function has a simpler appearance. The

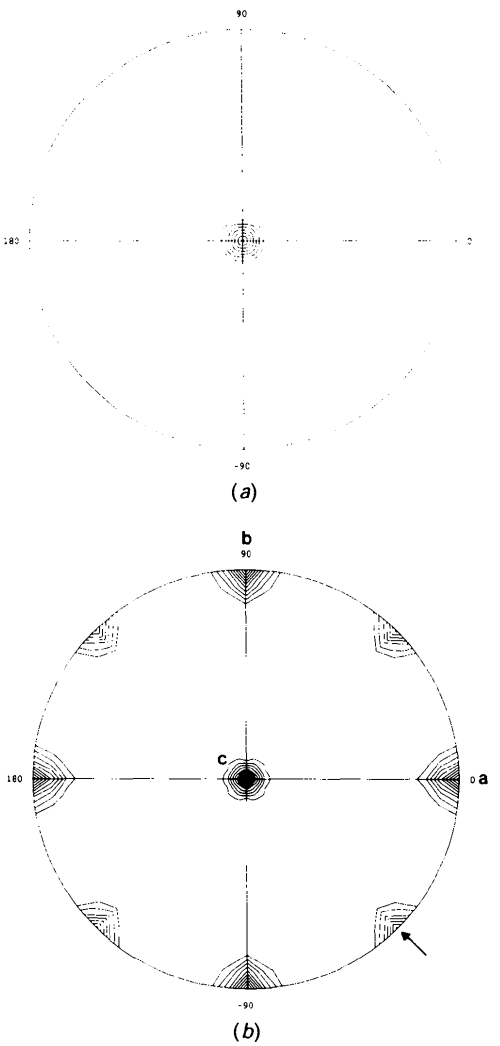

Fig. 2. Polar plots for sections $\chi = 90{\cdot}0$ (*a*) and $\chi = 180{\cdot}0$ (*b*) of a self-rotation map. Resolution range 3·3–20·0 Å and Patterson radius 18·0 Å, using *E*'s as amplitudes and a 5·0 step size. Contour levels are in units of $1{\cdot}0\sigma$, starting at $3{\cdot}0\sigma$.

Table 1. *Peaks in self-rotation*

Selected peaks found for a resolution range of 3·3–20·0 Å and a Patterson radius as indicated, using a 5·0° step size in the three polar angles. For 21 Å the maximum resolution is 3·6 Å. Amplitudes used are E's. ΔS(ignal)/σ indicates the height of each peak in r.m.s. units, relative to the highest 'noise' peak. Peak 0 represents the origin.

				$\Delta S/\sigma$		
Peak	θ	φ	χ	15·0 Å	18·0 Å	21·0 Å
0	0·0	0·0	0·0	6·7	9·8	10·6
1	180·0	Any	90·0	3·9	6·4	7·2
2	90·0	45·0	180·0	3·9	6·4	7·2

$\beta B2$-dimer model was created from the I structure by taking half the tetramer with 222 symmetry leaving out the domains underneath the PR plane (Fig. 1*c*), resulting in a dimer comprised of two γ-like monomers. The expectation was that the subunits in the C form would still interact very similarly around the PQ and QR interfaces, and that therefore this rigid γ-like dimer or half-tetramer constituted a reasonable model. On the other hand rigid-body movements around the connecting peptides in the PR interface may well be expected as they are not supported by tertiary interactions.

The γ-like dimer possessed a twofold axis along z. Whereas the dimer is in a $P1$ cell, the monomer is in a $P2$ cell. Any rotation-function solution peak will therefore be accompanied by a second peak at $\gamma + 180°$ in the $P1$ cell, when using Crowther's fast rotation function, where the first rotation is γ around z, showing the symmetry in the search molecule. Because of the presence of a pseudo fourfold in the C form there will be expected from the first found peak a second one at $\alpha + 90°$ on the same β section, keeping in mind that the last rotation is α around z, showing the symmetry in the target. The result will be a quartet of peaks on roughly the same β section of the cross-rotation function with the $P1$ cell.

Table 2. *Peaks in cross-rotation with γ-like $\beta B2$ dimer search molecule*

Peaks found for a resolution range of 3·3–20·0 Å and a Patterson window of 6·0–18·0 Å, using a 2·5° step size in the three Eulerian angles. Amplitudes used are E's. $\Delta(\alpha + \gamma)$ is given for the pairs $B2$–$A2$ and $B1$–$A1$, while $\Delta\gamma$ is given for the pairs $A1$–$A2$ and $B1$–$B2$. ΔS(ignal)/σ indicates the height of each peak in r.m.s. units, relative to the highest noise peak.

Peak	α	β	γ	$\Delta S/\sigma$	$(\alpha+\gamma)$	$\Delta(\alpha+\gamma)$	$\Delta\gamma$
A2	73·7	6·0	11·0	3·3	84·7		
B2	178·7	2·5	1·3	2·3	177·4	92·7	
A1	73·7	6·0	191·0	3·3	264·7		180·0
B1	177·5	3·0	180·0	2·3	357·5	92·8	178·7

Using E's in a resolution shell of 3·3–20·0 Å, this pattern was indeed found (Fig. 3, Table 2). The maximum difference in β is 3·5°. The perfect twofold along z shows up within the error of the step size used. The pseudo fourfold shows up with an angle of approximately 93°. The twofold in the search molecule halves the Eulerian cell dimension along γ. The cross-rotation space group $Pbc2_1$ ($\alpha = 180$, $\gamma = 360°$) (Moss, 1985) for two dimers per asymmetric unit therefore reduces to pseudo-rotation space group $Pbm2$ ($\alpha = 180$, $\gamma = 180°$) for two dimers per asymmetric unit. The pseudo fourfold in the target halves the cell along α. For one dimer per asymmetric unit the cell then becomes $Pbm2$ ($\alpha = 90$, $\gamma = 180°$).

Determination of the translation parameters

Having found the two rotation-function solutions for C-form $\beta B2$, T_2 translation functions were calculated. In space group $C222$, clear single solutions were found in the crystallographic translation function, both for dimers $A1$ and $B1$ (Fig. 4, Table 3). For dimer $B1$ the first peak was 6·3σ above the next-highest peak. Results were even better for dimer $A1$, where the next one differed by 11·6σ. The solution for dimer B was used for further translation

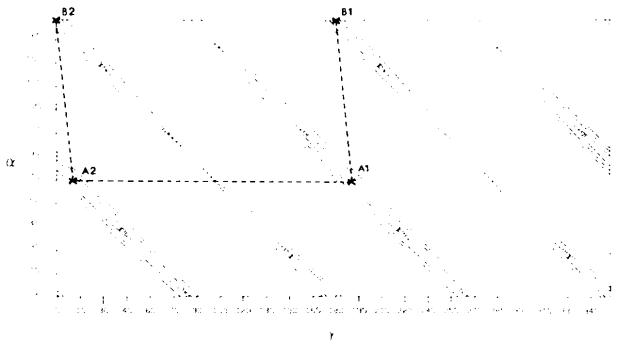

Fig. 3. Section $\beta = 5·0°$ of a cross-rotation map with γ-like $\beta B2$ dimer as the search model. Resolution range 3·3–20·0 Å and Patterson window 6·0 18·0 Å, using E's as amplitudes, and a 2·5° step size. Contour levels are in units of 1·0σ, starting at 3·0σ.

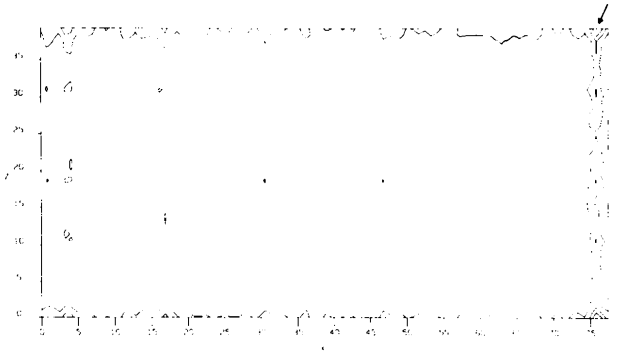

Fig. 4. Section $Y = 37·5$ Å of a translation function for dimer $B1$, with the position of dimer $A1$ unknown. Resolution range is 3·3–20·0 Å, using a 0·8 Å step size. The axes are marked in Å units. Contour levels are in units of 3·0σ. Shown is the asymmetric unit.

Table 3. *Peaks in translation functions with γ-like βB2 dimer search molecule*

Translation peaks found for a resolution range of 3·3–20·0 Å, using a 0·8 Å step size. Mol shows the dimer for which the translation function is computed; the numbers refer to the solutions of the cross-rotation. Function shows the step in the procedure, where C is the crystallographic and NC the non-crystallographic translation function. SUM is the sum of both. In brackets is shown whether the position of the second dimer is known in a step and therefore its crystallographic intermolecular vectors are subtracted. $\Delta S/\sigma$ indicates the height of each peak relative to the next-highest one in r.m.s. units, within brackets the height relative to the 20th peak, not counting symmetry equivalents. For SUM the second line shows the values when the pseudo-symmetry equivalents arising from C are excluded. x, y and z are coordinates found for the translation vectors in fractions of the unit cell.

Mol	Function		x	y	z	$\Delta S/\sigma$
*B*1	C	(*A*1 unknown)	0·491	0·224	−0·002	6·3 (8·9)
*A*1	NC	(*B*1 known)	0·214	0·002	0·499	18·1 (18·9)
*A*1	C	(*B*1 known)	0·215	0·003	0·497	10·9 (13·1)
*A*1	SUM	(*B*1 known)	0·215	0·003	0·497	17·6 (24·2)
						22·1 (24·2)
*A*1	C	(*B*1 unknown)	0·215	0·003	0·003	11·6 (14·5)

functions. In the non-crystallographic (NC) translation function, the highest peak was $18{\cdot}1\sigma$ above the next one (Fig. 5, Table 3). In the crystallographic function (C) this was $10{\cdot}9\sigma$. When summing (SUM) the crystallographic and non-crystallographic translation functions for *A*1 on the same origin as *B*1, the solution peak was $17{\cdot}6\sigma$ above the second peak, and $22{\cdot}1\sigma$ when excluding the peaks due to the symmetry equivalents from *C*. Therefore, the summation led to a significantly lower background level, when these pseudo-equivalents were excluded. The results clearly show how the new T_2 function singles out the correct origin out of a choice of four.

The resulting solution was examined graphically for an acceptable packing. There were no packing conflicts and atomic contacts appeared to be sensible. The results suggest that the dimer used for Patterson searches is indeed very similar to that found in the *C* form.

In space group $C222_1$ for *B*1 with *A*1 unknown no single peak stood out. The difference between the top peak and the next one was $0{\cdot}4\sigma$, and still only $3{\cdot}4\sigma$ with the 20th peak. Similarly for *A*1 with *B*1 unknown a solution could not be found. Here the first peak is $2{\cdot}7\sigma$ above the next one, and $7{\cdot}0\sigma$ above the 20th. As no solutions were found for either *A*1 or *B*1, calculations were discontinued. This result confirms that the space group is $C222$ and not $C222_1$.

It is interesting to compare the signal-to-noise ratios from the rotation function with those of the translation function. Assuming that all unexplained peaks in the rotation functions represent noise, the $\Delta S/\sigma$ varies from 2·3–3·3 for the cross-rotation, 3·9–7·2 for the self-rotation, and 6·3–22·1 for the translation functions. The self-rotation is presumably artificially high because of vector overlap. These data confirm that the rotation-function result is inherently less reliable than that of the translation function (Fujinaga & Read, 1987).

Initial refinement

For the refinement a molecule was considered to be comprised of two domains interacting with their γ-type interdomain *PQ* interface (Fig. 1*c*). For the molecular replacement solution initially the six rigid-body parameters for each of the four molecules in the asymmetric unit were refined at low resolution to allow for errors introduced by the fixed dimer model (Table 4). The resolution was then extended to 4·0 Å

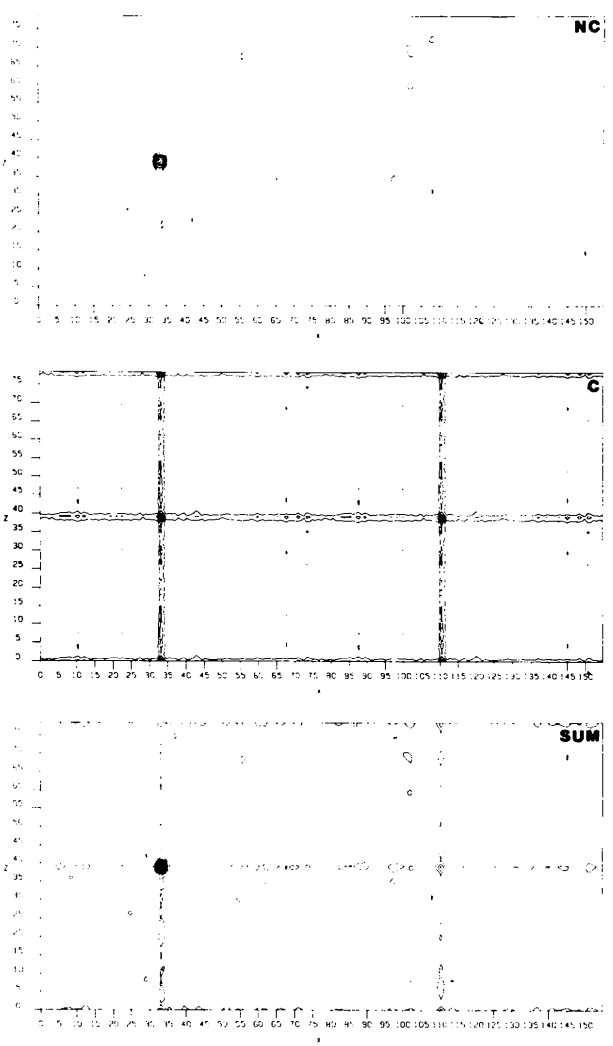

Fig. 5. Section $Y = 0{\cdot}8$ Å of a translation function for dimer *A*1, with the position of dimer *B*1 known. Resolution range, step size, contouring and marking are as in Fig. 4. NC shows one asymmetric unit of the non-crystallographic part, C four asymmetric units of the crystallographic part and SUM one asymmetric unit of the summation of these two parts.

Table 4. *Initial refinement of C-form βB2-crystallin with γ-monomer type asymmetric units*

For refinement the least-squares program *RESTRAIN* (Haneef *et al.*, 1985; Driessen *et al.*, 1989) was used. In each cycle the overall temperature factor was refined. No sigma cutoffs were applied. Note that neither N- and C-terminal extensions, nor connecting peptide were present during refinement. The four rigid bodies correspond to four γ-like subunits, the eight rigid bodies to the eight domains in the asymmetric unit.

Mode	Cycles	Resolution	Reflections	*R* factor
4 rigid bodies	4	9·0 20·0	737	39·7
4 rigid bodies	3	7·0 20·0	1617	41·7
4 rigid bodies	4	7·0 10·0	1102	41·3
4 rigid bodies	3	6·0 10·0	2051	42·0
4 rigid bodies	3	4·7 10·0	4818	38·6
4 rigid bodies	2	4·3 10·0	6416	37·7
4 rigid bodies	1	4·0 10·0	8071	37·1
8 rigid bodies	2	4·0–10·0	8071	36·8
8 rigid bodies + Restrained	2	3·7 10·0	10 255	35·2
Restrained	6	3·5 10·0	12 163	31·1
Restrained	4	3·3 10·0	14 356	30·4

to give a total r.m.s. shift of 0·92 Å. For each molecule the interdomain constraint was relaxed for eight rigid-bodies refinement, followed by constrained-restrained refinement. Restrained refinement alone, with extension of the resolution, gave the final model with an *R* factor of 30·4% at 3·3 10·0 Å. The total r.m.s. shift was 0·96 Å with respect to the molecular replacement solution. Individual domains within dimer *B*1 had rotated by as much as 3·6–4·4°, and by 1·9–3·0° within dimer *A*1.

Packing

The initial $2F_o - F_c$ electron density map showed good connectivity for all subunits, and confirmed the correctness of the molecular replacement solution. However, the density for a γ-type connecting peptide was broken, and both $2F_o - F_c$ and $F_o - F_c$ maps showed the same extended connecting peptide as seen in the *I*-form dimer, thus independently confirming the unexpected findings for that crystal form (Bax *et al.*, 1990). The asymmetric units were then converted from γ to β type. For ease of description the subunits were renamed *A*, *B*, *C* and *D* (with *A* and *B* subunits corresponding to rotation-function solution *B*1, and *C* and *D* to solution *A*1).

The four subunits in a tetramer are still related by 222 symmetry as in Fig. 1(*c*), which is now only approximate. There are two types of tetramer, one built up from two *AB* dimers around a crystallographic twofold parallel to the *y* axis at $z = 0$ (Fig. 7*c*), which is equivalent to the *R* axis in Fig. 1(*c*), and the other from two *CD* dimers around a twofold axis parallel to *x* at $z = \frac{1}{2}$, also equivalent to the *R* axis. Ignoring the centring, the centroids of the *AB* tetramers are at (0·0, 0·277, 0·0), (0·5, 0·223, 0·0) and of the *CD* tetramers at (0·219, 0·0, 0·5) and (0·281, 0·5, 0·5). The new contacts in the *C* form are caused by interactions between *AB* and *CD* tetramers in the asymmetric unit. Thus, the 'tetramer' within the asymmetric unit does not have 222 symmetry. Instead, two dimers (or tetramers) are related by a pseudo fourfold along *z* or a pseudo 2_1 axis parallel to the diagonals at *x*, $y = x + \frac{1}{4}$, $z = \frac{1}{4}$ or *x*, $y = -x + \frac{1}{4}$, $z = \frac{1}{4}$.

For the initially refined coordinates the non-crystallographic symmetry was examined in a preliminary way using all 700 main-chain atoms per subunit. The internal axis *Q* in the γ-like *AB* dimer does not appear to deviate significantly from a twofold axis (*ca* 0·35 Å r.m.s. for *AcBn*/*B′cA′n*) (Fig. 6*a*). This axis has been rotated 6·8° away from the *z* axis in the *xz* plane with a small translation of 0·3 Å along the *P* axis of the tetramer. The *P* axis is a near perfect twofold with a screw component of 0·6 Å (*AcBnB′cA′n*/*BcAnA′cB′n*). The deviation from a twofold axis for internal axis *Q* for the γ-like *CD*

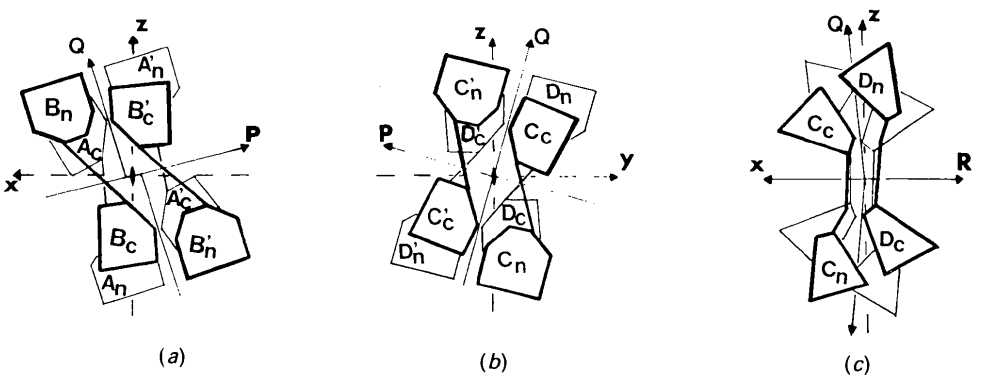

Fig. 6. Schematic representation of the *βB2* C222 tetramers. Domains are shown as wedges, and labeled as N- or C-terminal. Molecules which are generated by crystallographic twofold axes are indicated with '. (*a*) View along the *R* axis of the *AB* tetramer (coinciding with the crystallographic twofold along *y* at $x = 0$, $z = 0$). (*b*) View along the *R* axis of the *CD* tetramer (coinciding with the crystallographic twofold parallel to *x* at $y = 0$, $z = \frac{1}{2}$). (*c*) View of the *CD* tetramer along the *y* direction.

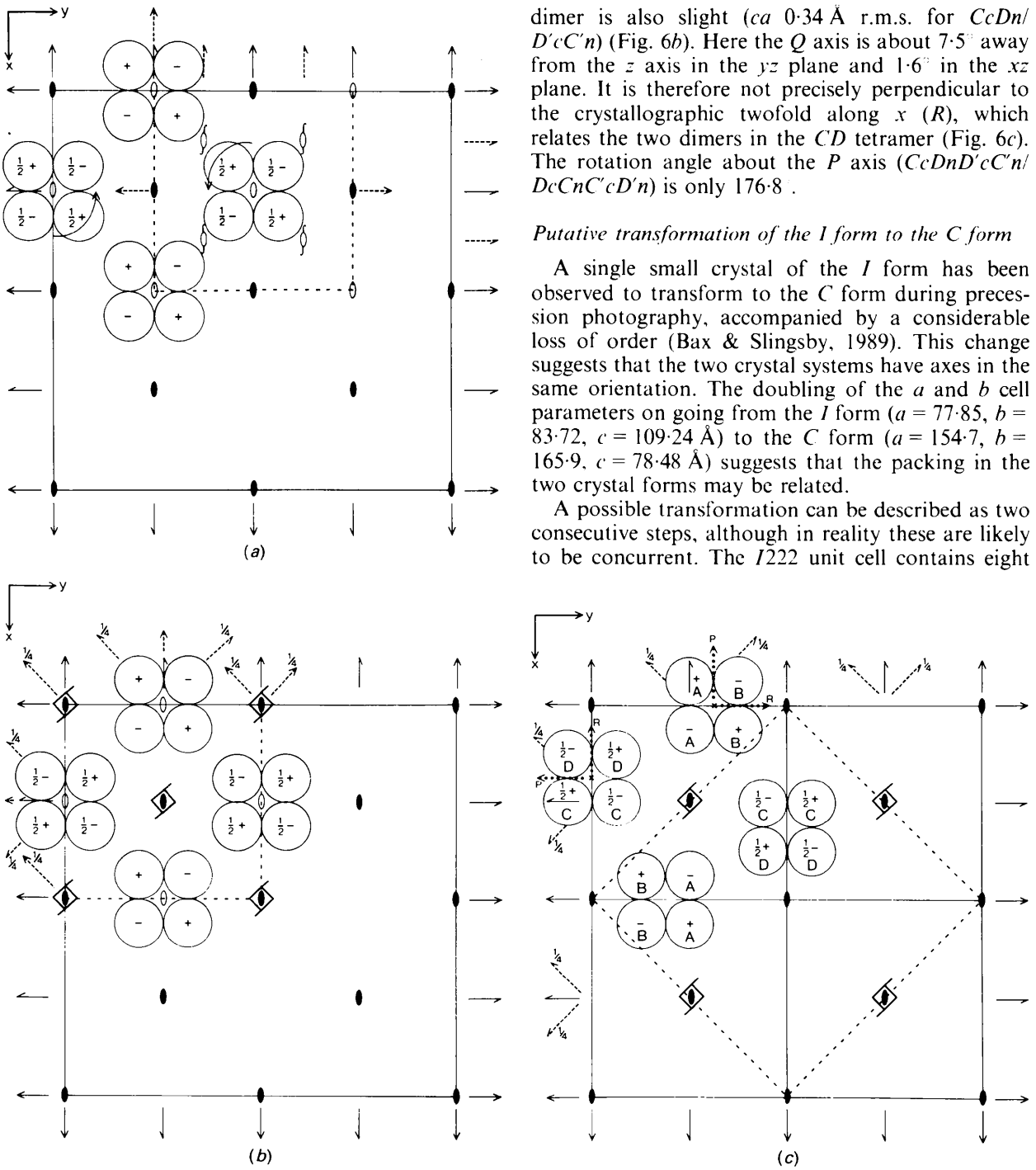

dimer is also slight (*ca* 0·34 Å r.m.s. for *CcDn/D'cC'n*) (Fig. 6*b*). Here the *Q* axis is about 7·5° away from the *z* axis in the *yz* plane and 1·6° in the *xz* plane. It is therefore not precisely perpendicular to the crystallographic twofold along *x* (*R*), which relates the two dimers in the *CD* tetramer (Fig. 6*c*). The rotation angle about the *P* axis (*CcDnD'cC'n/DcCnC'cD'n*) is only 176·8°.

Putative transformation of the I form to the C form

A single small crystal of the *I* form has been observed to transform to the *C* form during precession photography, accompanied by a considerable loss of order (Bax & Slingsby, 1989). This change suggests that the two crystal systems have axes in the same orientation. The doubling of the *a* and *b* cell parameters on going from the *I* form ($a = 77{\cdot}85$, $b = 83{\cdot}72$, $c = 109{\cdot}24$ Å) to the *C* form ($a = 154{\cdot}7$, $b = 165{\cdot}9$, $c = 78{\cdot}48$ Å) suggests that the packing in the two crystal forms may be related.

A possible transformation can be described as two consecutive steps, although in reality these are likely to be concurrent. The *I*222 unit cell contains eight

Fig. 7. Transformation of *I*222 to *C*222. Schematic unit cells are shown with subunits drawn as circles, which have been grouped in tetramers. For clarity contacts between tetramers are not depicted. (*a*) Packing of subunits (one per asymmetric unit) in space group *I*222 ($a = 77{\cdot}85$, $b = 83{\cdot}72$, $c = 109{\cdot}24$ Å) which is indicated by dashed lines (tightly spaced for symmetry operators) and open symbols where different from *C*222 ($a = 154{\cdot}7$, $b = 165{\cdot}9$, $c = 78{\cdot}48$ Å). *C*222 is indicated by solid lines and black symbols. The arrows show the rotation of 90° of tetramers at $(\frac{1}{2}, \frac{1}{2}, \frac{1}{2})$ to transform to (*b*). (*b*) Packing of subunits (one per asymmetric unit) in the hypothetical space group $P4_222$ ($a = 80$, $b = 80$, $c = 109$ Å) which is indicated by dashed lines and open symbols where different from *C*222. Translations along *z*, and to a lesser extent along *x* and *y* transform to (*c*). (*c*) Packing of subunits (two per asymmetric unit) in the pseudo space group $P4_22_12$ ($a = b = 113$, $c = 78{\cdot}48$ Å) which is indicated by dashed lines and open symbols where different from *C*222. Superimposed is the real space group *C*222 (four subunits per asymmetric unit, labeled *A*, *B*, *C* and *D*). The dotted lines show the local *P* and *R* axes for each tetramer.

subunits, one per asymmetric unit. Initially, the central crystallographic tetramer of the *I* cell (which will become the *CD* tetramer in the *C* cell) undergoes a radical rotation of 90° around *z*, while the tetramer on the corner (which will become the *AB* tetramer) does not change (Fig. 7*a*). A *CD* tetramer in a neighbouring cell rotates in the opposite direction. This leads to a hypothetical, but unobserved $P4_22$ cell with cell dimensions $a = b = 80$, $c = 109$ Å (Fig. 7*b*). The twofold axes parallel to *z* at $x = 0$, $y = \frac{1}{2}$ and $x = \frac{1}{2}$, $y = 0$ in the *I* cell now become fourfolds. The *AB* and *CD* tetramers are crystallographic and completely equivalent at this stage. Each tetramer still has perfect 222 symmetry. However, this situation is unlikely to give good lattice contacts. In the next step better contacts are provided by a small fractional translation of +0·031 along *x* for the central *CD* tetramer and a translation of +0·027 along *y* for the *AB* tetramer. At the same time the tetramers slide past each other parallel to *z*, which causes the cell dimension to shrink from 109 to 78·5 Å, a decrease of 27%. The fourfolds on the corners of the $P4_22$ cell are lost, as are the three intersecting twofolds at $x = \frac{1}{2}$, $y = 0$ and $x = 0$, $y = \frac{1}{2}$. The initial result is a $P4_22_12$ cell with $a = b = 113$, $c = 78{\cdot}48$ Å and $\gamma = 93°$, and with a dimer in the asymmetric unit (Fig. 7*c*). The dimers in a tetramer are related by crystallographic twofolds parallel to *x* and *y*, while the monomers in a dimer are now related by non-crystallographic twofolds. Contacts between *AB* tetramers and *CD* tetramers are largely between *A* and *D* subunits and between *B* and *C* subunits (Fig. 7*c*). With rigid-body movements around the extended connecting peptides, these contacts are non-equivalent, so that tetramers are related by a rotation of approximately 87 and 93°. Thus the cell is *C*222 rather than $P4_22_12$, with four subunits in the asymmetric unit.

The contacts will be described in detail elsewhere. Refinement is in progress. The current *R* factor for all data between 3·3 and 8·0 Å is 21%.

Scanning was performed at Imperial College, University of London, by courtesy of Dr A. Wonacott and Professor D. Blow. We thank Professor T. L. Blundell for stimulating discussions. HD acknowledges support from the European Molecular Biology Organisation.

References

Bax, B., Lapatto, R., Nalini, V., Driessen, H., Lindley, P. F., Mahadevan, D., Blundell, T. L. & Slingsby, C. (1990). *Nature (London)*, **347**, 776–780.

Bax, B. & Slingsby, C. (1989). *J. Mol. Biol.* **208**, 715–717.

Berbers, G. A. M., Hoekman, W. A., Bloemendal, H., de Jong, W. W., Kleinschmidt, T. & Braunitzer, G. (1984). *Eur. J. Biochem.* **139**, 467–479.

Blundell, T., Lindley, P., Miller, L., Moss, D., Slingsby, C., Tickle, I., Turnell, B. & Wistow, G. (1981). *Nature (London)*, **289**, 771–777.

*CCP*4 (1979). *The SERC (UK) Collaborative Computing Project*, No. 4. *A Suite of Programs for Protein Crystallography*. SERC Daresbury Laboratory, Warrington, England.

Chirgadze, Y. N., Nevskaya, N. A., Fomenkova, N. P., Nikonov, S. V., Serggeev, Y. V., Brazhnikov, E. V., Garber, M. B., Lunin, V. Y., Urzumtsev, A. P. & Vernoslova, E. A. (1986). *Dokl. Akad. Nauk SSSR*, **290**, 492–495.

Crowther, R. A. (1972). *The Molecular Replacement Method*, edited by M. G. Rossmann, pp. 173–178. New York: Gordon & Breach.

Crowther, R. A. & Blow, D. M. (1967). *Acta Cryst.* **23**, 544–548.

Driessen, H., Haneef, M. I. J., Harris, G. W., Howlin, B., Khan, G. & Moss, D. S. (1989). *J. Appl. Cryst.* **22**, 510–516.

Fox, G. C. & Holmes, K. C. (1966). *Acta Cryst.* **20**, 886–891.

French, G. S. & Wilson, K. S. (1978). *Acta Cryst.* A**34**, 517–525.

Fujinaga, M. & Read, R. J. (1987). *J. Appl. Cryst.* **20**, 517–521.

Haneef, I., Moss, D. S., Stanford, M. J. & Borkakoti, N. (1985). *Acta Cryst.* A**41**, 426–433.

Harada, Y., Lifchitz, A., Berthou, J. & Jolles, P. (1981). *Acta Cryst.* A**37**, 398–406.

Leslie, A. G. W., Brick, P. & Wonacott, A. T. (1986). *Daresbury Laboratory Information Quarterly for Protein Crystallography*, Vol. 18, pp. 33–39. SERC Daresbury Laboratory, Warrington, England.

Moss, D. S. (1985). *Acta Cryst.* A**41**, 470–475.

Nixon, P. E. & North, A. C. T. (1976). *Acta Cryst.* A**32**, 320–325.

Read, R. J. & Schierbeek, A. J. (1988). *J. Appl. Cryst.* **21**, 490–495.

Slingsby, C., Driessen, H. P. C., Mahadevan, D., Bax, B. & Blundell, T. L. (1988). *Exp. Eye Res.* **46**, 375–403.

Slingsby, C., Miller, L. R. & Berbers, G. A. M. (1982). *J. Mol. Biol.* **157**, 191–194.

Ten Eyck, L. F. (1973). *Acta Cryst.* A**29**, 183–191.

Tickle, I. J. (1985). *Proceedings of the Daresbury Study Weekend*, edited by P. A. Machin, pp. 22–26. Daresbury: SERC.

Tollin, P. (1966). *Acta Cryst.* **21**, 613–614.

Tollin, P. (1969). *Acta Cryst.* A**25**, 376–377.

Vagin, A. A. (1989). *Joint CCP4 and ESF-EACBM Newsletter on Protein Crystallography*, edited by K. Henrick & K. Wilson, pp. 117–121. SERC Daresbury Laboratory, Warrington, England, and EMBL, Hamburg, Germany.

Wang, D., Driessen, H. P. C. & Tickle, I. J. (1991). *J. Mol. Graphics*, **9**, 38, 50–52.

White, H. E., Driessen, H. P. C., Slingsby, C., Moss, D. S. & Lindley, P. F. (1989). *J. Mol. Biol.* **207**, 217–235.

White, H. E., Driessen, H. P. C., Slingsby, C., Moss, D. S., Turnell, W. G. & Lindley, P. F. (1988). *Acta Cryst.* B**44**, 172–178.

Whittaker, E. T. & Watson, G. N. (1927). *A Course of Modern Analysis*, p. 182. Cambridge Univ. Press.

Wilson, C. C. & Tollin, P. (1988). *Acta Cryst.* A**44**, 226–230.

Winkler, F. K., Schutt, C. E. & Harrison, S. C. (1979). *Acta Cryst.* A**35**, 901–911.

Wistow, G., Slingsby, C., Blundell, T., Driessen, H., de Jong, W. & Bloemendal, H. (1981). *FEBS Lett.* **133**, 9–16.

Wistow, G., Turnell, B., Summers, L., Slingsby, C., Moss, D., Miller, L., Lindley, P. & Blundell, T. (1983). *J. Mol. Biol.* **170**, 175–202.